



Acclimation of C₂C₁₂ myoblasts to physiological glucose concentrations for *in vitro* diabetes research

Jacob Dohl, Jonathan Foldi, Julian Heller, Heath G. Gasier, Patricia A. Deuster, Tianzheng Yu*

Consortium for Health and Military Performance, Department of Military and Emergency Medicine, Hébert School of Medicine, Uniformed Services University of the Health Sciences, Bethesda, MD 20814, USA

ARTICLE INFO

Keywords:

Obesity
Diabetes mellitus
Hyperglycemia
Hyperlipidemia
Myoblasts
Skeletal muscle
Cellular model
Mitochondria
Reactive oxygen species

ABSTRACT

Aims: The interplay between hyper-glycemia and -lipidemia in diabetes mellitus (DM) is important in simulating diabetic conditions. However, cell culture media typically contain supraphysiological levels of glucose to stimulate cellular growth, which also desensitizes cells to elevated glucose levels. Moreover, creating hyperlipidemic conditions *in vitro* requires specialized carriers because unbound lipids form micelles when introduced to liquid media. This study sought to develop a novel method for simulating DM conditions *in vitro*.

Materials and methods: We acclimated the C₂C₁₂ mouse myoblasts to culture medium with 5.6 mM glucose, which mimics physiological levels, and created a bovine serum albumin-palmitic acid conjugate for lipid transport to explore the effects of hyperlipidemia. We simulated diabetic conditions *in vitro* by using both hyper-glycemic and -lipidemic conditions and compared the results to that of only hyperglycemic or hyperlipidemic conditions.

Key findings: Acclimated cells exposed to these hyper-glycemic (15 mM glucose) and/or -lipidemic (0.25 mM palmitate) conditions for 2 h showed increased mitochondrial fragmentation and membrane potential as well as elevated reactive oxygen species production compared to control cells. These findings suggest altered mitochondrial morphology and function, which have been confirmed using isolated rat flexor digitorum brevis myofibers. Hyper-glycemic and/or -lipidemic stimulations for 24 h significantly increased mitogen-activated protein kinase kinase MEK 1/2 protein expression, upregulated the early pro-apoptotic transcription factor C/EBP homologous protein (CHOP), and induced apoptosis.

Significance: Our results further support and confirm the utility of this method which will allow for subsequent investigations studying the effects of hyper-glycemia and/or -lipidemia *in vitro*.

1. Introduction

Diabetes mellitus (DM) is a global health issue with an estimated 422 million people diagnosed with diabetes worldwide, and this number is expected to continue increasing [1]. The American Diabetes Association defines normoglycemia as a fasting plasma glucose < 5.6 mM, and DM ≥ 6.5 mM [2]. Patients with DM also tend to present with lipoprotein abnormalities including, but not limited to, hyperlipidemia [3,4]. Consideration should thus be given to both glycemic and lipoprotein metabolic complications when designing experiments aimed at understanding the pathophysiology of DM.

Investigators utilizing *in vivo* animal models to examine the mechanisms of DM typically increase lipid concentrations in the chow and/or employ special rodent strains (e.g. Lep^{ob/ob} or Zucker Fatty rats)

that easily develop hyper-glycemia and -lipidemia [5–7]. Although these methods are important for advancing our understanding of DM, animal studies have significant limitations, including cost, experiment duration, and inter-individual variability. *In vitro* studies can generally be performed with a fraction of the time and cost, but they also face obstacles of their own. For instance, supraphysiological levels of glucose without lipids are the baseline in typical cellular media. In particular, Dulbecco's Modified Eagle Medium (DMEM) has a concentration of 25 mM glucose, a 400% increase from normal physiology, to promote and accelerate cellular growth. Although the very high concentration is effective in accelerating growth rates, the cells also become desensitized to any additional glucose, as is evident in documented metrics of insulin production from pancreatic β cells and/or the decrease in insulin-stimulated protein kinase B activation of adipocytes exposed to

* Corresponding author at: Consortium for Health and Military Performance, Department of Military and Emergency Medicine, Hébert School of Medicine, Uniformed Services University of the Health Sciences, 4301 Jones Bridge Road, Bethesda, MD 20814, USA.

E-mail address: tianzheng.yu.ctr@usuhs.edu (T. Yu).

<https://doi.org/10.1016/j.lfs.2018.09.041>

Received 2 July 2018; Received in revised form 19 September 2018; Accepted 21 September 2018

Available online 22 September 2018

0024-3205/ © 2018 Elsevier Inc. All rights reserved.

large amounts of glucose *in vitro* [8,9]. This limitation is especially important for studies that focus on the slight increases in glucose concentration indicative of diabetes. In studying DM, it would be far more useful to be able to acclimate various types of cells to a physiological concentration of glucose.

The interplay between hyper-glycemia and -lipidemia in DM is also important in simulating diabetic conditions. Treating cells with fatty acids in liquid media is a challenge since hydrophobic fatty acids form into micelles, which prevent them from being transported into the cells. In nature, albumins, a class of globular proteins found in blood serum, serve to transport a range of hydrophobic molecules, including fatty acids, hormones, and bilirubin [10]. Bovine serum albumin (BSA), a staple in many laboratories, is able to transport palmitic acid both *in vitro* and *in vivo* and has been identified as an ideal vehicle for transporting fatty acids into cells [11,12].

Based on the problems associated with DM investigations *in vitro*, this study sought to develop a novel method for simulating DM conditions *in vitro*. Since skeletal muscle is a major insulin-responsive organ critical for maintaining glucose levels within the body [13,14], we first selected to study C₂C₁₂ mouse myoblasts. Once the myoblasts were acclimated to a physiological level of glucose (5.6 mM) in DMEM, they were introduced to high glucose (HG), high fat (HF), or both high glucose and high fat (HGHF) conditions in order to fully simulate DM conditions. We then assessed for mitochondrial morphology and function and levels of oxidative stress, which are purported to be associated with the pathogenesis of DM and its complications [15–17]. Next, we used our new method to conduct additional studies with isolated rat myofibers from the flexor digitorum brevis (FDB). Finally, we examined the chronic effects of HG and/or HF on stress signaling pathways and apoptotic cell death. In conjunction, these studies were designed to better understand the effects of hyper-glycemia and -lipidemia - both separately and in combination - as occurs in DM, on mitochondrial morphology and function, reactive oxygen species (ROS) production, stress signaling pathways, and cell injury in both a cell and tissue model.

2. Materials and methods

2.1. BSA-conjugated palmitate protocol

This BSA-conjugated palmitate protocol was adapted from the Agilent Seahorse (https://www.agilent.com/cs/library/usermanuals/public/XF_Palmitate_BSA_Substrate_Quickstart_Guide.pdf, last accessed on August 27, 2018), with alterations to meet our purposes. BSA is a complex protein that contains six main binding sites for long-chain fatty acids as well as numerous weak tertiary binding sites [18]. To maximize transport into cells, we used a 6:1 palmitic acid to BSA ratio. BSA (final concentration of 0.17 mM; Fisher Bioreagents, Cat. No. BP9703100) was added to 5.6 mM low glucose (LG) DMEM (LG DMEM, ThermoFisher Scientific, Cat. No. 11885-084), incubated at 37 °C, and continuously stirred until dissolution. Half of the LG DMEM solution containing BSA was diluted at a 1:1 ratio with fresh LG DMEM and the final pH was adjusted to 7.4 prior to sterilization by filtering through a Corning® 250 mL Filter Unit. Concurrently, 2.5 mM of palmitic acid (Sigma-Aldrich, Cat. No. P0500) was added to a different flask containing fresh LG DMEM and stirred continuously at 70 °C. Upon dissolution, the palmitic acid solution was added in 5 mL increments to the remaining BSA solution at a 2:5 dilution with gentle stirring. After incubating this solution at 37 °C with gentle stirring for 1 h, LG DMEM was added to increase the total volume to be equal to that of the BSA stock solution. The pH was then adjusted to 7.4 and the solution was filtered for sterility: the end result was the BSA-Conjugated Palmitate Solution. The final concentration of the BSA-conjugated palmitate solution was 0.17 mM BSA conjugated with 1 mM palmitate.

2.2. C₂C₁₂ cell culture

C₂C₁₂ mouse myoblasts (ATCC® CRL-1772™) were initially cultured in 25 mM high glucose (HG) DMEM supplemented with 10% Fetal Bovine Serum (FBS), 100 units/mL penicillin, and 100 µg/mL streptomycin. To acclimate cells to physiological levels of glucose, the HG DMEM was replaced with 5.6 mM low glucose (LG) DMEM and cells were allowed to grow undisturbed for several weeks until they reached a stable growth rate. All cells were cultured at 37 °C with 5% CO₂ in a humidified incubator and passaged every 2–3 days to maintain a confluency below 60% and prevent differentiation.

2.3. Rat flexor digitorum brevis myofibers isolation

All procedures involving animals were approved by Uniformed Services University of the Health Sciences Institutional Animal Care and Use Committee. Sprague Dawley rats (Charles River, Germantown, MD) aged 20–24 weeks were euthanized using isoflurane. The FDB muscles from both feet were harvested, dissected of visible connective tissue without mechanically disrupting the myofibers, and incubated in LG DMEM containing 3 mg/mL collagenase and 1 mg/mL dispase at 37 °C in a 5% CO₂ humidified incubator for ~2–3 h. After digestion, the muscles were removed from the LG DMEM with collagenase and dispase and placed in a new dish with only LG DMEM. Fiber bundles were then gently triturated by using glass pipettes and separated into individual fibers that were isolated into a third dish containing only LG DMEM. From this third dish, aliquots of isolated myofibers were transferred to dishes containing LG DMEM supplemented with 0.2% BSA and 0.1% gentamicin (w/v) and allowed to recover at 37 °C in a 5% CO₂ humidified incubator. All myofibers were harvested and isolated on the day of the experiments.

2.4. Quantification of cell growth rates

Cells were counted automatically with a Bio-Rad TC20 Cell Counter (Hercules, CA) and verified manually under a Nikon Eclipse Ti-E light microscope operated by NIS-Elements Viewer (Nikon, Tokyo, Japan) at room temperature. The means of each day were then used for final evaluation.

2.5. High-glucose and/or high-fat cell treatment

C₂C₁₂ cells were plated on petri dishes with cover glass at a confluence of ~40%. D-glucose was dissolved in PBS at a concentration 2.5 M and sterilized by filtration. For HG treatment, 4 µL of 2.5 M glucose stock solution was added per 1 mL medium. High fat (HF) treatment was performed by mixing 1 mM BSA-conjugated palmitate stock solution with LG DMEM at a ratio of 1:4. HGHF treatment combined the two treatments, treating with fats followed by glucose. The final culture concentrations were 0.25 mM palmitate and/or 15 mM glucose. This treatment has been previously used by us and others to mimic DM hyper-glycemia and -lipidemia in cultured cells [19–21]. C₂C₁₂ cells or FDB myofibers treated with BSA stock solution (HF control) and PBS (HG control) were used as vehicle controls. Our preliminary results show that BSA solution, PBS, or BSA and PBS combined treatment did not alter mitochondrial function or cell viability.

2.6. Determination of mitochondrial morphology, function and ROS production

C₂C₁₂ cells and rat FDB myofibers were stained with the following fluorescent dyes (ThermoFisher Scientific, Waltham, MA): 1) 100 nM of MitoTracker™ Red CMXRos (Cat. No. M7512) was used to assess mitochondrial morphology; 2) as a surrogate of mitochondrial function, mitochondrial membrane potential ($\Delta\Psi_m$) was determined using 100 nM tetramethylrhodamine, ethyl ester (TMRE) (Cat. No. T669); 3)

ROS, primarily superoxide anion ($\cdot\text{O}_2^-$) were determined by monitoring the oxidation of $5\ \mu\text{M}$ dihydroethidium (DHE) (Cat. No. D23107) as described previously [22]. For ROS measurements in rat FDB myofibers, 5–6 nuclei were manually circled in each fiber and mean value of the DHE fluorescence intensity was used as the representative data of this fiber. A total of 20 fibers was quantified in each treatment.

2.7. Fluorescent microscopy

All imaging was performed at room temperature with a Nikon Eclipse Ti-E light microscope operated by NIS-Elements Viewer software (Nikon, Tokyo, Japan). Excitation/emission wavelengths were as follows: MitoTracker™ Red (579/599), TMRE (555/579), DHE (500/588). Fluorescent imaging for mitochondrial morphology was achieved using a $20\times$ objective, whereas $\Delta\Psi\text{m}$ and ROS imaging occurred with a $10\times$ objective. All images were captured with the same exposure time and digital gain in each experiment, and further modified and analyzed utilizing ImageJ software (NIH, Bethesda, MD).

2.8. Caspase 3/7 and Annexin V assays

Caspase 3/7 activities were measured by CellEvent™ Caspase-3/7 Green detection reagent (Invitrogen, MA), per manufacturer's instruction. Dead cells were detected by using an Annexin V Alexa Fluor® 488 apoptosis kit (Invitrogen, MA), as we reported previously [23].

2.9. Western blotting

A total of $10\ \mu\text{g}$ of protein from cell lysate was loaded to gels and separated by SDS-PAGE gel electrophoresis. Western blotting was performed with the primary antibodies against CHOP and MEK 1/2. GAPDH was used as a loading control. Secondary antibodies were horseradish peroxidase-conjugated anti-mouse or anti-rabbit antibodies. All the antibodies were purchased from Cell Signaling Technology (Danvers, MA). The bands were visualized with Western ECL Blotting Substrates (Bio-Rad, CA) and images were acquired using a Bio-Rad ChemiDoc MP Imaging System. Western blot densitometry analysis was performed using ImageJ software (NIH, MD).

2.10. Statistical analysis

All experiments were repeated at least three times independently. Values are means \pm SD. Mean group differences were determined by using *t*-test (2 groups) or ANOVA (> 2 groups), with values of $p \leq 0.05$ being considered statistically significant.

3. Results

3.1. Acclimation of C_2C_{12} cells to physiological levels of glucose

Growth rates were initially diminished in C_2C_{12} cells after the medium was changed from HG DMEM to LG DMEM (data not shown). After a two-month acclimation period C_2C_{12} cells cultured in either LG DMEM or HG DMEM appeared similar. Both appeared typical of mouse myoblasts, which suggests no significant cellular alterations following acclimation to LG DMEM. Cell growth rates over a three-day period were also similar, although there was greater variability among overall cell numbers in LG DMEM cells (Fig. 1A & B).

3.2. HG and/or HF treatment induces mitochondrial fragmentation in C_2C_{12} cells

Fig. 2A demonstrates visualization of the mitochondrial network as an index of mitochondrial fitness [15]. Control cells acclimated to physiological levels of glucose (LG) had thin, moderately long, tubular

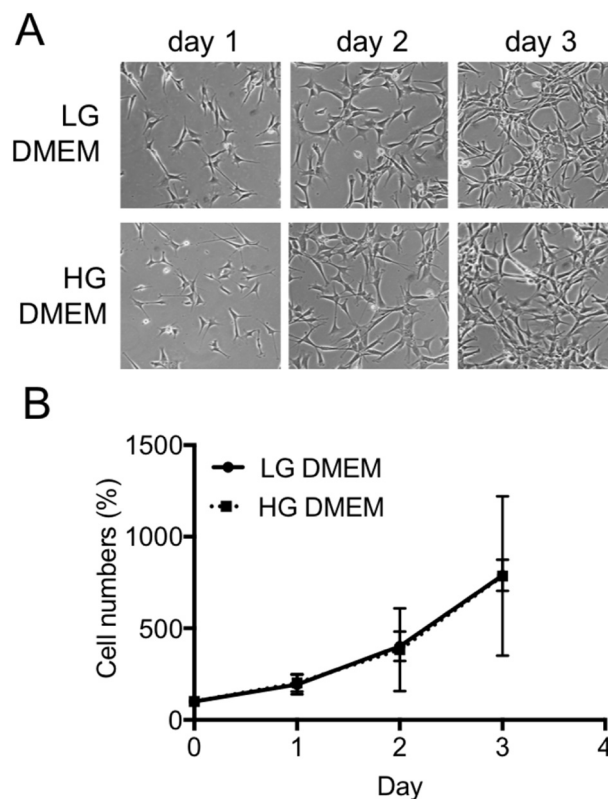


Fig. 1. Acclimation of C_2C_{12} cells to physiological levels of glucose. A, representative bright light microscope images of C_2C_{12} mouse myoblasts grown in either “normal” DMEM containing 25 mM glucose (HG DMEM), or DMEM containing physiological levels of glucose (5.6 mM glucose, LG DMEM). Both cell types are visually similar and are representative of typical mouse myoblasts, suggesting no significant cellular alterations following acclimation to LG DMEM. B, cells were counted in order to evaluate overall growth rates after acclimation to LG DMEM. Cell growth, determined over a three-day period, was similar, although there was greater variability between cell numbers in LG DMEM cells.

mitochondria arranged in a coherent network, with small amounts of disjointed mitochondria in the periphery of the cell. In comparison, HG cells showed shorter, punctate mitochondria with a moderately intact mitochondrial network. The mitochondrial mass of HF and HGHF cells showed increased fragmentation relative to control cells, coupled with a pronounced globular shape, no coherent network, and increased mitochondrial isolation. The percentages of cells containing short/fragmented mitochondria in HG were significantly higher than in control cells, but lower than in HF or HGHF cells (Fig. 2B).

3.3. HG and/or HF increases $\Delta\Psi\text{m}$ in C_2C_{12} cells

To assess mitochondrial function, we stained C_2C_{12} cells with TMRE, a positively-charged fluorescent dye that accumulates within the mitochondrial matrix dependent upon $\Delta\Psi\text{m}$. HG treated cells showed a moderate but significant increase in $\Delta\Psi\text{m}$ compared to control cells (Fig. 3A & B). The increases in $\Delta\Psi\text{m}$ in HF and HGHF treated cells were larger and more robust than that in HG cells (Fig. 3A & B).

3.4. HG and/or HF elevates ROS levels in C_2C_{12} cells

Increased production of ROS, which may cause an imbalance in the redox state, is recognized as a major cause of the clinical complications associated with diabetes and obesity [15,24]. We measured cellular ROS levels by the increased ethidium fluorescence from the oxidation of DHE in C_2C_{12} cells treated with HG, HF, or HGHF. As depicted in

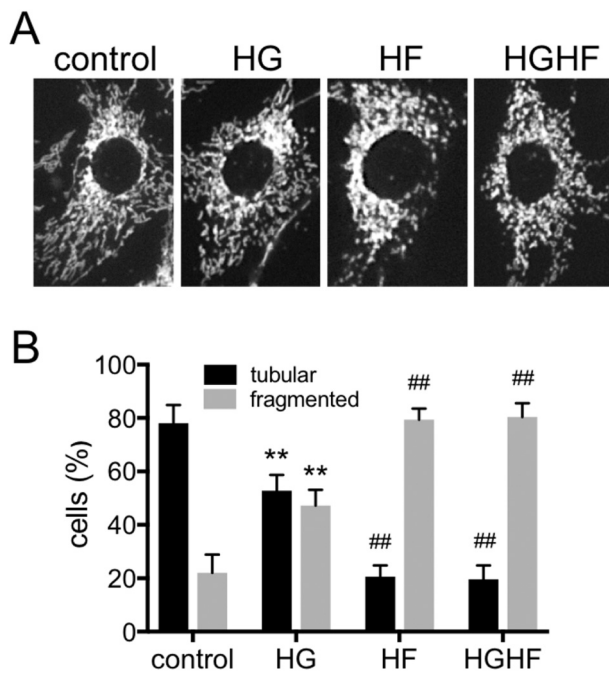


Fig. 2. Comparison of effects of HG, HF and HGHF on mitochondrial morphology in C_2C_{12} cells. A, representative fluorescent microscopy images of C_2C_{12} cells labeled with MitoTracker™ Red. These cells were maintained in medium containing 5.6 mM glucose and treated for 2 h with 15 mM glucose (HG), 0.25 mM palmitate (HF), or combination of high glucose and high fat (HGHF); control were the cells treated with PBS and BSA solution. B, quantification of the percentages of cells with tubular or short/fragmented mitochondria. 300–400 cells were counted in each treatment. ** $p < 0.01$ vs. control, ## $p < 0.01$ vs. HG.

Fig. 4A & B, HG treatment significantly increased ROS production, consistent with our previous findings [19,22,25]. Similar to the mitochondrial morphology and membrane potential data (Figs. 2 and 3), HF and HGHF –induced ROS production were significantly higher than in HG cells (Fig. 4A & B).

3.5. HGHF induces mitochondrial deformation, increases membrane potential and ROS production in rat FDB myofibers

Mice and rats are the two most common species used in diabetes research; they both develop DM in a way that resembles the pathophysiology in humans [5,26]. Due to a larger FDB muscle size in rats than in mice, it is relatively easy to harvest a large amount of high-quality rat myofibers. To confirm the results obtained from experiments with C_2C_{12} myoblasts, we isolated rat FDB myofibers and subjected them to the HGHF treatment described above. Mitochondria in control fibers were organized, distinct bands evenly distributed throughout the fibers (Fig. 5A). In contrast, mitochondria in HGHF treated fibers were disorganized and more irregular, which suggests altered mitochondrial morphology (Fig. 5A). As with C_2C_{12} myoblasts, $\Delta\Psi_m$ and ROS production were significantly higher in the HGHF treated fibers compared to control fibers (Fig. 5B–D).

3.6. HG and/or HF activates stress signaling pathways and induces apoptosis in C_2C_{12} cells

We finally examined the chronic effects (24 h treatment) of HG and/or HF on intracellular stress signaling pathways and apoptotic cell death in C_2C_{12} cells. HG, HF, or HGHF treatments all significantly increased MAP kinase MEK 1/2 protein expression (Fig. 6A & B). The C/EBP homologous protein (CHOP), an early pro-apoptotic transcription factor, was also upregulated in cells treated with HF or HGHF (Fig. 6A &

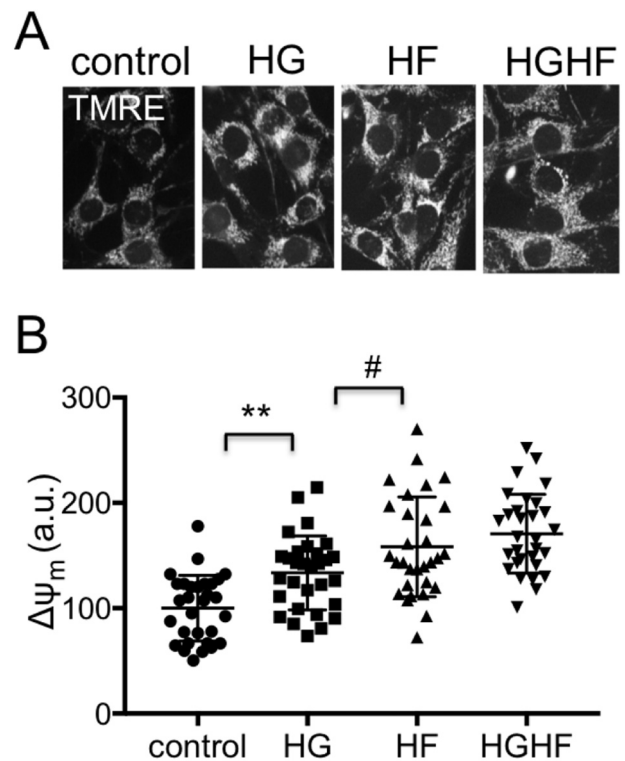


Fig. 3. Comparison of effects of HG, HF and HGHF on mitochondrial membrane potential ($\Delta\Psi_m$) in C_2C_{12} cells. A, representative fluorescent microscopy images of C_2C_{12} cells stained with TMRE, a $\Delta\Psi_m$ fluorescent indicator. These cells were maintained in medium containing 5.6 mM glucose and treated for 2 h with 15 mM glucose (HG), 0.25 mM palmitate (HF), or combination of high glucose and high fat (HGHF); control were the cells treated with PBS and BSA solution. B, quantification of TMRE fluorescence intensity. 40 cells were randomly selected in each treatment for quantification, and experiments were performed three times, independently. ** $p < 0.01$ vs. control, ## $p < 0.01$ vs. HG.

B). Consistent with these results, HG, HF, and HGHF treatments for 24 h induced caspase 3/7 activation and apoptosis in C_2C_{12} cells (Fig. 6C & D). The numbers of apoptotic cells were significantly higher in combined HG and HF treatment than those treated with HG or HF alone (Fig. 6D).

4. Discussion

Hyper-glycemia and -lipidemia are hallmark features of DM [15,17]. The primary difficulties in replicating those conditions *in vitro* relate to the makeup of standard media: in particular, supraphysiological levels of glucose, which lead to cellular desensitization, and the absence of a lipid transporter. This study was undertaken to address these concerns in order to more accurately mimic DM conditions *in vitro*. Our results indicate that this can be accomplished through two sequential steps: (1) transfer of C_2C_{12} myoblasts from HG DMEM, containing 25 mM glucose, to a modified DMEM, containing 5.6 mM physiological glucose concentration, followed by a two-month acclimation period; and (2) creation of a BSA-lipid conjugate that allows for effective addition of lipids to the medium and subsequent transport to cells. Establishing this novel *in vitro* method has allowed us to perform various experiments aimed at studying the effects of energy surplus indicative of DM on mitochondrial morphology and function, and ROS production.

A proposed mechanism for the progression of DM *in vivo* is that cycles of hyper-glycemia and -lipidemia lead to mitochondrial damage and increased ROS production, which together reduce the cell's capacity to respond to an energy surplus [15,16,27]. Diabetes is known to be

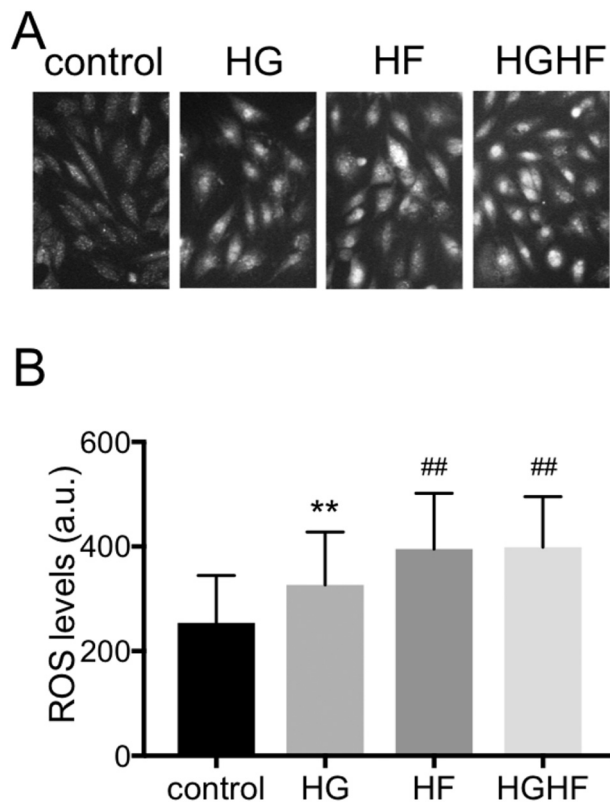


Fig. 4. Comparison of effects of HG, HF and HGHF on reactive oxygen species (ROS) levels in C₂C₁₂ cells. A, representative fluorescent microscopy images of C₂C₁₂ cells labeled with the ROS indicator DHE. These cells were maintained in medium containing 5.6 mM glucose and treated for 2 h with 15 mM glucose (HG), 0.25 mM palmitate (HF), or combination of high glucose and high fat (HGHF); control were the cells treated with PBS and BSA solution. B, cellular ROS levels were quantified by measuring DHE fluorescence intensity. 40 cells were randomly selected in each treatment. ***p* < 0.01 vs. control, ##*p* < 0.01 vs. HG.

associated with generalized mitochondrial dysfunction: mitochondrial deformation and small, fragmented mitochondria have been reported in obese and diabetic patients [15,28,29], animal models [30–32], and cultured cells [19,22,32]. Imbalances in fission and fusion rates can result in increased mitochondrial fragmentation, a known precursor to cytochrome C release and eventual apoptosis [33]. In addition, increased ROS production, recognized as a major cause of the clinical complications associated with obesity and diabetes [15], has also been shown to increase strain on mitochondria and contribute to mitochondrial dysfunction. Our results indicate that those pathophysiological mechanisms can be created *in vitro* in either myoblasts or adult myofibers. Supplying excess energy in the form of glucose and saturated fatty acids *via* our novel method resulted in mitochondrial fragmentation along with increases in the mitochondrial membrane potential and ROS production.

In addition to mitochondrial impairment and ROS overproduction, DM has been shown to activate intracellular stress signaling pathways and cause apoptotic cell injuries [15,25,34]. In this study, we found that hyper-glycemic and/or -lipidemic stimulation increased protein expression of MEK 1/2 and induced apoptosis in C₂C₁₂ myoblasts. MEK 1/2 phosphorylates and activates the extracellular signal-regulated kinases (ERK 1/2), and MEK-ERK signals regulate various cellular processes such as survival and apoptosis [35]. We previously reported that ERK 1/2 phosphorylates the mitochondrial fission protein dynamin related protein 1 (Drp1) and induces the activation of mitochondrial fission and ROS production [36]. Therefore, MEK-ERK signals activated by hyper-glycemia and/or -lipidemia, result in mitochondrial fragmentation and ROS production acutely but cell injury over the long-term. Our results suggest that similar mechanisms are induced in cultured myoblasts through the application of our hyper-glycemic and/or -lipidemic stimulations *in vitro*: MEK-ERK signals are upregulated 24 h after the treatments, along with a corresponding increase in CHOP expression, caspase 3/7 activation, and apoptotic cell death.

In vitro studies currently utilize either primary or immortalized cell lines. We used an immortalized C₂C₁₂ cell line and worked with its undifferentiated myoblast form. However, our method of simulating DM conditions by using glucose and BSA-conjugated palmitate can be applied to either primary or immortalized cell lines, both before and after differentiation. Primary cells are generally more biologically relevant for simulating *in vivo* conditions; but they are expensive, often

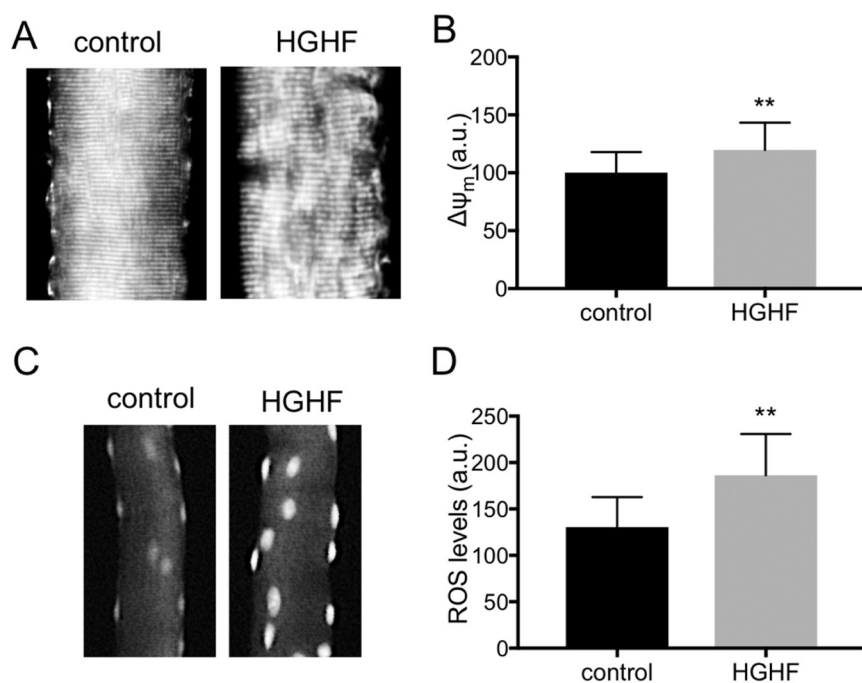


Fig. 5. HGHF induces mitochondrial deformation, increases mitochondrial membrane potential and ROS production in rat skeletal muscle fibers. A, representative fluorescent microscopy images of rat FDB myofibers labeled with MitoTracker™ Red: mitochondria in control fibers appear in distinct bands evenly distributed throughout the fiber while HGHF treated fibers are disorganized and more irregular. B, mitochondrial membrane potential ($\Delta\Psi_m$) was quantified by TMRE fluorescence intensity: $\Delta\Psi_m$ was significantly increased in HGHF fibers. 40 fibers were randomly selected in each treatment and experiments were repeated three times, independently. ***p* < 0.01 vs. control. C, DHE was oxidized by ROS and localized within the nuclei of the fibers, creating multiple areas of fluorescence in each fiber; HGHF fibers had consistently higher DHE fluorescence in each of their nuclei compared to those of control fibers. D, quantification of ROS levels in fibers showed a significant increase of ROS in HGHF treated fibers compared to control. 20 fibers were quantified in each treatment and experiments were repeated three times, independently. ***p* < 0.01 vs. control.

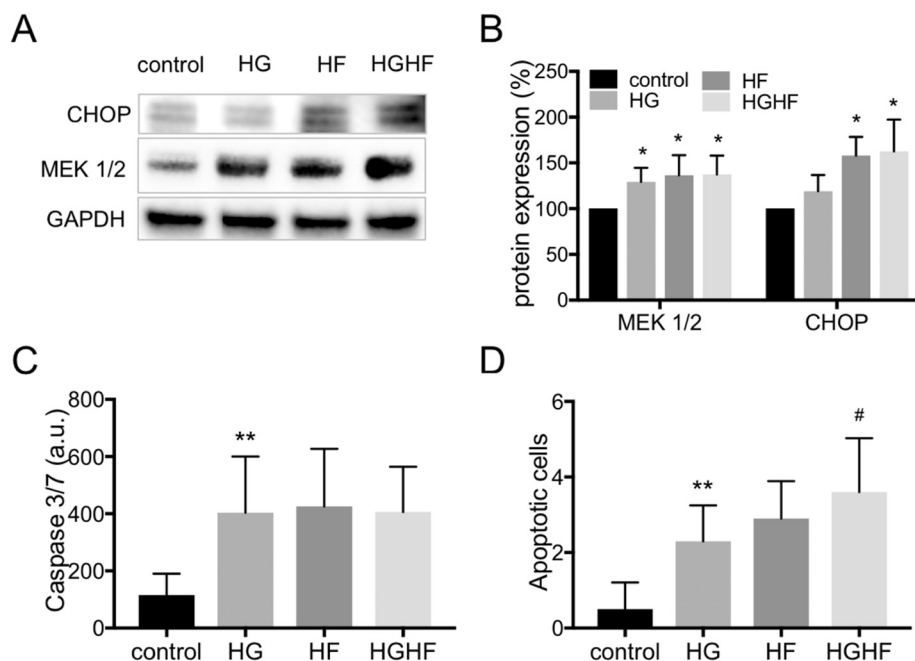


Fig. 6. Chronic effects of HG, HF or HGHF on stress signaling pathways and apoptotic cell death in C_2C_{12} cells. A, representative western blots of C_2C_{12} cells treated for 24 h with 15 mM glucose (HG), 0.25 mM palmitate (HF), or combination of high glucose and high fat (HGHF). B, quantified results of the western blots. Experiments were repeated at least 3 times independently, data were presented as % to control cells. * $p < 0.05$ vs. control. C, Caspase 3/7 activities were increased in cells treated with HG, HF, or HGHF for 24 h. $n = 40$ in each group, * $p < 0.05$ vs. control. D, apoptotic cell death was detected by Annexin V cell surface labeling. Annexin V positive cells were counted in 20 fields in each group, * $p < 0.05$ vs. control, # $p < 0.05$ vs. HG; experiments were repeated 3 times.

difficult to obtain, and challenging to work with. Immortalized cell lines can be a cost-effective alternative as long as they are well maintained and verified to ensure there is no major genetic drift, cross contamination, or misidentification [37].

Despite the range of applicability with various cell lines, the use of cells *in vitro* has limitations in and of itself. There is a short time frame of use for both immortalized cells and primary cell lines with our method; acclimated C_2C_{12} myoblasts can readapt to hyper-glycemic and -lipidemic conditions after a prolonged incubation time, namely during experimentation lasting several days, and primary myofibers, after repeated passaging, are likely to become senescent; these properties limit the window of use for both cell types [38,39]. In addition, both primary and immortal cell lines are studied in isolation and cannot replicate the complex conditions of *in vivo* experiments. Cells cultured *in vitro* lack communication with various cell types, which is common and important in biological conditions. This also limits their reactions to treatment as well as being separated from the hormonal systems also important in cellular signaling. Despite the strengths of this method and *in vitro* studies in general, they are not without their own limitations.

Observing the differences in hyperglycemia, hyperlipidemia, and a combination of hyper-glycemia and -lipidemia is useful for determining the changes in energy metabolism in health and DM. Fats and carbohydrates are the principal substrates that fuel mitochondrial respiration for ATP synthesis, and resting muscle prefers fatty acids as fuel [40,41]. Our results show that, in C_2C_{12} myoblasts, HG exposure results in mild increases in ROS production and membrane potential, as well as a shift towards shortened and punctate mitochondria as compared to control myoblasts. However, HF exposure induced a much larger increase in ROS production and membrane potential as well as extensive mitochondrial fragmentation. HGHF treatment resulted in highly similar outcomes as the HF treatment alone, and lacked any potentiation from the combination of HG and HF. It is known that fatty acid oxidation can inhibit whole body glucose oxidation *in vivo* and similar effects may be occurring *in vitro* in this instance, with the surplus of fatty acids inhibiting the consumption of glucose and mediating the effects of HG exposure [42,43]. Importantly, our HF exposure only included palmitic acid, a ubiquitous saturated fatty acid. Further efforts should examine potential differences due to changes in fatty acid combinations, for example long chain omega 3 and omega 6 as well as monounsaturated and possibly short or medium chain fatty acids. What effects would

these lipids have on mitochondrial function and morphology?

In summary, we have presented a novel method for simulating hyper-glycemic and -lipidemic conditions in C_2C_{12} mouse myoblasts and isolated rat FDB myofibers. This is a convenient method for conducting *in vitro* DM research without sacrificing its major advantages. Combining hyper-glycemic and -lipidemic conditions *in vitro* more closely replicates what is documented *in vivo*. Acclimating cells to normoglycemic conditions can be accomplished in two to three months, and cells can then be stored in liquid nitrogen to avoid the need for re-acclimation. Conjugation of a fatty acid to BSA is both easily accomplished and more economical than purchasing commercially available pre-conjugated lipids. We hope that our *in vitro* model can be adopted for further study of DM with the goal of advancing our understanding of mechanisms involved to develop improved prevention and treatment strategies.

Conflicts of interest

The authors declare no conflict of interest. The views expressed are those of the authors and do not reflect the official position of the Uniformed Services University of Health Sciences, the United States Navy or the Department of Defense.

Acknowledgments

We thank Kristin Heitman for critical reading. This work was supported by the Defense Health Program Center Alliance for Nutritional and Dietary Supplement Research HU0001-14-1-003.

References

- [1] Collaboration, N.C.D.R.F., Worldwide trends in diabetes since 1980: a pooled analysis of 751 population-based studies with 4.4 million participants, *Lancet* 387 (10027) (2016) 1513–1530.
- [2] A. American Diabetes, Diagnosis and classification of diabetes mellitus, *Diabetes Care* 33 (Suppl. 1) (2010) S62–S69.
- [3] S.L. Abbate, J.D. Brunzell, Pathophysiology of hyperlipidemia in diabetes mellitus, *J. Cardiovasc. Pharmacol.* 16 (Suppl. 9) (1990) S1–S7.
- [4] I.J. Goldberg, Clinical review 124: diabetic dyslipidemia: causes and consequences, *J. Clin. Endocrinol. Metab.* 86 (3) (2001) 965–971.
- [5] A.J. King, The use of animal models in diabetes research, *Br. J. Pharmacol.* 166 (3) (2012) 877–894.
- [6] K. Srinivasan, et al., Combination of high-fat diet-fed and low-dose streptozotocin-

- treated rat: a model for type 2 diabetes and pharmacological screening, *Pharmacol. Res.* 52 (4) (2005) 313–320.
- [7] S. Skovso, Modeling type 2 diabetes in rats using high fat diet and streptozotocin, *J. Diabetes Invest.* 5 (4) (2014) 349–358.
- [8] B. Brock, et al., Glucose desensitization in INS-1 cells: evidence of impaired function caused by glucose metabolite(s) rather than by the glucose molecule per se, *Metabolism* 51 (6) (2002) 671–677.
- [9] K.A. Robinson, M.G. Buse, Mechanisms of high-glucose/insulin-mediated desensitization of acute insulin-stimulated glucose transport and Akt activation, *Am. J. Physiol. Endocrinol. Metab.* 294 (5) (2008) E870–E881.
- [10] T. Peters Jr., *All About Albumin: Biochemistry, Genetics, and Medical Applications*, Academic press, 1995.
- [11] T.U. Yardimci, A. Aktulga-Gursoy, O.N. Ulutin, Palmitic acid transport in platelets of normal subjects and of patients with liver cirrhosis, *Acta Haematol.* 63 (1) (1980) 2–6.
- [12] E.J. Demant, G.V. Richieri, A.M. Kleinfeld, Stopped-flow kinetic analysis of long-chain fatty acid dissociation from bovine serum albumin, *Biochem. J.* 363 (Pt 3) (2002) 809–815.
- [13] K.F. Petersen, G.I. Shulman, Pathogenesis of skeletal muscle insulin resistance in type 2 diabetes mellitus, *Am. J. Cardiol.* 90 (5) (2002) 11–18.
- [14] A. Shemyakin, et al., Regulation of glucose uptake by endothelin-1 in human skeletal muscle in vivo and in vitro, *J. Clin. Endocrinol. Metab.* 95 (5) (2010) 2359–2366.
- [15] Y. Yoon, et al., Mitochondrial dynamics in diabetes, *Antioxid. Redox Signal.* 14 (3) (2011) 439–457.
- [16] M.K. Hesslink, V. Schrauwen-Hinderling, P. Schrauwen, Skeletal muscle mitochondria as a target to prevent or treat type 2 diabetes mellitus, *Nat. Rev. Endocrinol.* 12 (11) (2016) 633–645.
- [17] L. Rochette, et al., Diabetes, oxidative stress and therapeutic strategies, *Biochim. Biophys. Acta* 1840 (9) (2014) 2709–2729.
- [18] A.A. Spector, K. John, J.E. Fletcher, Binding of long-chain fatty acids to bovine serum albumin, *J. Lipid Res.* 10 (1) (1969) 56–67.
- [19] T. Yu, et al., Mitochondrial fission mediates high glucose-induced cell death through elevated production of reactive oxygen species, *Cardiovasc. Res.* 79 (2) (2008) 341–351.
- [20] S.K. Jain, et al., Low levels of hydrogen sulfide in the blood of diabetes patients and streptozotocin-treated rats causes vascular inflammation? *Antioxid. Redox Signal.* 12 (11) (2010) 1333–1337.
- [21] C. Yang, et al., Mitochondrial dysfunction in insulin resistance: differential contributions of chronic insulin and saturated fatty acid exposure in muscle cells, *Biosci. Rep.* 32 (5) (2012) 465–478.
- [22] T. Yu, J.L. Robotham, Y. Yoon, Increased production of reactive oxygen species in hyperglycemic conditions requires dynamic change of mitochondrial morphology, *Proc. Natl. Acad. Sci. U. S. A.* 103 (8) (2006) 2653–2658.
- [23] T. Yu, P. Deuster, Y. Chen, Role of dynamin-related protein 1-mediated mitochondrial fission in resistance of mouse C₂C₁₂ myoblasts to heat injury, *J. Physiol.* 594 (24) (2016) 7419–7433.
- [24] T. Nishikawa, E. Araki, Impact of mitochondrial ROS production in the pathogenesis of diabetes mellitus and its complications, *Antioxid. Redox Signal.* 9 (3) (2007) 343–353.
- [25] T. Yu, et al., Curcumin induces concentration-dependent alterations in mitochondrial function through ROS in C₂C₁₂ mouse myoblasts, *J. Cell. Physiol.* (2018) 1–11, <https://doi.org/10.1002/jcp.27370>.
- [26] A. Al-Awar, et al., Experimental diabetes mellitus in different animal models, *J. Diabetes Res.* 2016 (2016) 9051426.
- [27] W.I. Sivitz, M.A. Yorek, Mitochondrial dysfunction in diabetes: from molecular mechanisms to functional significance and therapeutic opportunities, *Antioxid. Redox Signal.* 12 (4) (2010) 537–577.
- [28] D.E. Kelley, et al., Dysfunction of mitochondria in human skeletal muscle in type 2 diabetes, *Diabetes* 51 (10) (2002) 2944–2950.
- [29] M. Liesa, M. Palacin, A. Zorzano, Mitochondrial dynamics in mammalian health and disease, *Physiol. Rev.* 89 (3) (2009) 799–845.
- [30] C.A. Galloway, et al., Transgenic control of mitochondrial fission induces mitochondrial uncoupling and relieves diabetic oxidative stress, *Diabetes* 61 (8) (2012) 2093–2104.
- [31] A. Makino, B.T. Scott, W.H. Dillmann, Mitochondrial fragmentation and superoxide anion production in coronary endothelial cells from a mouse model of type 1 diabetes, *Diabetologia* 53 (8) (2010) 1783–1794.
- [32] H.F. Jheng, et al., Mitochondrial fission contributes to mitochondrial dysfunction and insulin resistance in skeletal muscle, *Mol. Cell. Biol.* 32 (2) (2012) 309–319.
- [33] R.J. Youle, A.M. van der Bliek, Mitochondrial fission, fusion, and stress, *Science* 337 (6098) (2012) 1062–1065.
- [34] S. Abdelli, et al., Intracellular stress signaling pathways activated during human islet preparation and following acute cytokine exposure, *Diabetes* 53 (11) (2004) 2815–2823.
- [35] Y.D. Shaul, R. Seger, The MEK/ERK cascade: from signaling specificity to diverse functions, *Biochim. Biophys. Acta* 1773 (8) (2007) 1213–1226.
- [36] T. Yu, B.S. Jhun, Y. Yoon, High-glucose stimulation increases reactive oxygen species production through the calcium and mitogen-activated protein kinase-mediated activation of mitochondrial fission, *Antioxid. Redox Signal.* 14 (3) (2011) 425–437.
- [37] G. Kaur, J.M. Dufour, Cell lines: valuable tools or useless artifacts, *Spermatogenesis* 2 (1) (2012) 1–5.
- [38] G. Ravenscroft, et al., Dissociated flexor digitorum brevis myofiber culture system—a more mature muscle culture system, *Cell Motil. Cytoskeleton* 64 (10) (2007) 727–738.
- [39] G. Shefer, Z. Yablonka-Reuveni, Isolation and culture of skeletal muscle myofibers as a means to analyze satellite cells, *Methods Mol. Biol.* 290 (2005) 281–304.
- [40] L. Storlien, N.D. Oakes, D.E. Kelley, Metabolic flexibility, *Proc. Nutr. Soc.* 63 (2) (2004) 363–368.
- [41] D.E. Kelley, L.J. Mandarino, Fuel selection in human skeletal muscle in insulin resistance: a reexamination, *Diabetes* 49 (5) (2000) 677–683.
- [42] P.J. Randle, Regulatory interactions between lipids and carbohydrates: the glucose fatty acid cycle after 35 years, *Diabetes Metab. Rev.* 14 (4) (1998) 263–283.
- [43] G. Boden, et al., Mechanisms of fatty acid-induced inhibition of glucose uptake, *J. Clin. Invest.* 93 (6) (1994) 2438–2446.